JOURNAL OF MAGNETIC RESONANCE IMAGING 34:173–183 (2011)

Original Research

Comparison of a 32-Channel with a 12-Channel Head Coil: Are There Relevant Improvements for Functional Imaging?

Evangelia Kaza, PhD,[1]* Uwe Klose, PhD,[2] and Martin Lotze, MD[1]

Purpose: To evaluate the suitability of a 12- or 32-channel head coil and of a prescan normalization filter for functional magnetic resonance imaging (fMRI) studies at different brain regions.

Materials and Methods: fMRI was obtained from 36 volunteers executing a visually instructed motor paradigm using a 12-channel head matrix coil and a 32-channel phased-array head coil with and without prescan normalization filtering at 3 T. The time-course signal-to-noise ratio (tSNR) and the magnitude of functional activation (beta-value, *t*-value, percent signal change) were statistically compared between experimental conditions for the contralateral primary motor and visual cortex, contralateral thalamus, and ipsilateral anterior cerebellar hemispheres.

Results: tSNR was higher overall measuring with the 32-channel array and with prescan normalization. Without filtering, the 32-channel array delivered higher functional activation magnitudes for the visual cortex, whereas the 12-channel array seemed superior in this respect in thalamus and cerebellum. Filtering did not considerably affect the fMRI-activation magnitude detected from the 12-channel coil; its application favored the 32-channel coil at the subcortical and cerebellar locations but disfavored it at the cortical ones.

Conclusion: The 32-channel coil detected more fMRI-activation cortically but less subcortically than the 12-channel coil; prescan normalization improved activation parameters only at central brain structures.

Key Words: 32-channel head coil; fMRI; tSNR; BOLD
J. Magn. Reson. Imaging 2011;34:173–183.

RECENT DEVELOPMENTS in radiofrequency (RF) coil design allow the construction of receiving array head coils with an increased number of individual elements, showing improvements of several characteristics of magnetic resonance imaging (MRI) quality. Theory predicts that phased arrays perform better in signal-to-noise ratio (SNR) terms than single coils, without sensitivity losses at larger distances (1). Nevertheless, signal cancellations (2) or no substantial SNR improvements with increasing number of coil elements at the center of multichannel coils have also been observed (3).

A 32-channel array head coil is reported to have exhibited substantial gains in SNR compared to an 8-channel coil (4) and an overall higher SNR and reduced noise amplification (g-factor) for accelerated imaging compared to a 12-channel coil at 3 T (5). Kahn et al (6) indicated that a 32-channel array detected a higher blood oxygenation level-dependent (BOLD) signal magnitude than a 12-channel array for high-resolution occipital cortical imaging at a field strength B_0 of 3 T. Fellner et al (7) indicated, albeit using a nonstandard functional MRI (fMRI) evaluation software and a small statistical sample, a higher BOLD detectability at the contralateral primary motor cortex (M1) but not at the ipsilateral M1 and supplementary motor area (SMA) at 1.5 T. Albrecht et al (8) recorded cortically higher SNR as well as additional fMRI activation at the SMA, supramarginal and postcentral gyrus, and ipsilateral cerebellum with a 32-channel coil compared to an 8-channel coil.

Up to now, no systematic group study covering the whole head has been conducted, investigating possible advantages of multichannel coils with a high number of receiving elements for fMRI with commonly used settings. Additionally, it would be interesting to select the optimal coil if there would be an effect of location which differs between coil types. Therefore, we investigated to which extent the increased number of receiving channels and close-fitting design of these coils have a positive effect in detecting the BOLD response in different brain areas on a well-described fMRI motor paradigm (visually presented finger-tapping task) with reported cortical, thalamic, and cerebellar representation sites (9,10) using a medium spatial resolution. We compared two commercial head coils, one with 32 and one with 12 receiving elements, focusing our interest on one apical and one occipital

[1]Functional Imaging Unit, Center of Diagnostic Radiology and Neuroradiology, University of Greifswald, Germany.
[2]MR Research Group, Department of Diagnostic and Interventional Neuroradiology, University Hospital Tübingen, Germany.
*Address reprint requests to: E.K., Friedrich-Loeffler Strasse 23a, D-17489 Greifswald, Germany. E-mail: evangelia.kaza@uni-greifswald.de
Received August 23, 2010; Accepted March 15, 2011.
DOI 10.1002/jmri.22614
View this article online at wileyonlinelibrary.com.

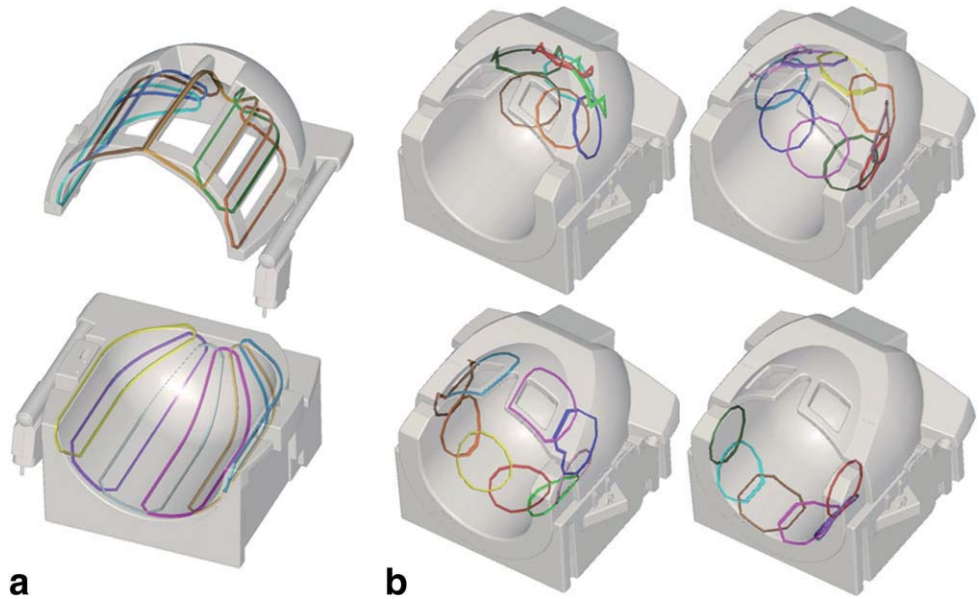

Figure 1. The two head coils compared in the present study and the layout of their individual RF receiving elements. **a**: 12-channel head matrix coil: its lower und upper part were symmetric and housed six RF receivers each. **b**: 32-channel phased-array head coil: 20 receivers were built on the lower and 12 on the upper part of the helmet. The RF elements had individual dimensions and were arranged in four parallel transverse planes (from top left to bottom right): top plane with seven elements, a circle of 10 elements, a row of nine elements and a bottom row of six elements. [Color figure can be viewed in the online issue, which is available at wileyonlinelibrary.com.]

cortical, one cerebellar and one thalamic region of highest expected activation. As these regions are not substantially affected by susceptibility artifacts and since our goal was to quantify possible differences in BOLD signal detection between the two arrays at the best, we refrained from using parallel imaging to avoid any BOLD sensitivity penalties, as reported (11,12).

In addition to assessing the fMRI sensitivity between head coils and filtering conditions we also inspected the time-course SNR (tSNR) characteristics of the activated brain regions. tSNR is a measure of image signal detectability over time that includes physiological noise contributions. Physiological noise becomes a substantial part of the total noise at 3 T (13), especially at a medium or low spatial resolution (14), and affects gray matter more than white matter (15). Due to these high noise contributions the expected SNR increase for a 32-channel coil (4) would not directly translate into improvements in fMRI sensitivity (16). Therefore, tSNR represents a more accurate predictor of BOLD detectability (17).

Phased-arrays exhibit an inhomogeneous reception pattern by having a stronger B1-sensitivity near their surface (18) that can even counteract the central brightening artifact at 3 T (19). For a higher number of receiving array elements the intensity increase in their vicinity becomes so pronounced that a B1 receive-field correction seems appropriate to an investigator interested in the whole sample or in regions located near the coil center. This is the case for a 32-channel head coil, which exhibits rising SNR from its center to its surface (4). Hence, we also investigated how the application of a commercial on-line signal homogenization filter affects the detected activation and the tSNR in all examined brain regions.

For the statistical assessment of the head coils characteristics we assumed an increased tSNR and BOLD response for the array with the higher number of receiving elements and for the application of a homogenization filter. As measures of activation we considered the outcome of an established fMRI analysis software (statistical parametric mapping; SPM), whereas we used various approaches in order to fortify the results of our comparison: a statistical analysis of the individual activation indicators over the whole population of the participants, both at individual voxels and over entire regions, as well as a group analysis at the second level of the SPM software. A similar statistical analysis of the first BOLD evaluation approach was conducted over the individual tSNR values, allowing for direct comparison between these measures for the different areas and experimental conditions.

MATERIALS AND METHODS

Devices and Subjects

A commercially available 12-channel head matrix coil and a commercially available 32-channel phased-array head coil were compared on a Siemens Verio 3.0 T whole body system (all three devices: Siemens Medical Solutions, Erlangen, Germany). The lower and upper parts of the head matrix coil were symmetrical and housed six partially overlapping RF receiving elements each (Fig. 1a). This coil had an inner vertical diameter of 26.0 cm and an inner horizontal diameter of 25.0 cm. RF receivers were about 32 cm long and their width amounted to about 7 cm at the inferior end, decreasing towards the superior end. The

neighboring elements of a coil component were geometrically decoupled. The 32 receiving channels of the second head coil were partially overlapping, arranged in a soccer-ball geometry in four parallel transverse planes (Fig. 1b). The RF elements had individual dimensions, with a mean loop diameter of 85 mm. The distance between the three adjacent bottom planes amounted to 60 mm, while the apical plane lay 15 mm farther than the second plane. The coil's inner dimensions were 23 cm in the vertical and 19.5 cm in the horizontal axis. In total, 20 out of the 32 individual channels were built on the lower part of the helmet.

A scanner-available prescan normalization filter which corrects the receiving coil inhomogeneities was also examined. This filtering method acquires low-resolution ("prescan") images over the maximum field of view (FOV) with the body coil, which is supposed to be homogeneous enough, and compares them to the images acquired by the surface coils. The resulting information is used to normalize the full-resolution images. This technique can compensate only for RF field inhomogeneities of the receiving coils.

We investigated 36 healthy volunteers (17 males, 19 females; age range 22.4–44.0 years; average age: 26.8 ± (SD) 4.1 years) using both coils and filter characteristics in a random temporal order. Written informed consent was obtained from all participants and the study was approved by the Ethics Committee of the local medical faculty.

Motor Task During Scanning

Subjects were asked to lie down in supine position on the scanner couch and their head was comfortably fixed with foamed plastic in the head coil in order to avoid involuntary movement during task execution. All participants performed with their right hand a sequential finger-tapping task of 12 simultaneously visually presented white numbers indicating button presses on a black background. These numbers ranged from 1 (index finger) to 4 (little finger), forming two different complex finger sequences consisting of 12 digits each ("easy": 4 3 1 2 1 1 2 1 4 3 1 3 and "difficult": 1 3 4 2 1 2 4 1 3 2 4 2). All subjects had practiced both number series prior to scanning for about 15 minutes on average, to achieve their individual errorless maximum tapping velocity. Visual stimuli (a finger sequence or a fixation cross) lasted 25 seconds each and were projected on a panel at the rear scanner end. Participants could view the entire projection without obstructions by looking straight at a double mirror, especially designed for each head coil and attachable on it at the same distance from the volunteer's eyes. Conditions were performed in a block design alternating rest (fixation cross) followed by the "easy" tapping sequence, then rest followed by the "difficult" sequence, so that each tapping sequence appeared three times in total. Finger-tapping was executed continuously on a LUMItouch optical response keypad (Photon control, Burnaby, Canada), as long as a number series was presented. The keypad was optically connected to the task-presenting computer, allowing recording of the subject's button press responses with Presentation (v. 12.2; Neurobehavioral Systems, Albany, CA).

fMRI Scanning Parameters

For each coil, a 2D echo-planar imaging (EPI) sequence was applied, with parameters: repetition time (TR) = 2.5 sec, echo time (TE) = 30 msec, flip angle $\alpha = 90^\circ$, FOV = 192 mm, matrix size = 64 × 64, readout bandwidth = 1662 Hz/pixel, echo spacing = 0.67 msec, and anterior-to-posterior phase-encoding direction. In all, 120 images, each comprising 34 slices of 3 mm thickness with 1 mm gap and orientation parallel to the line connecting the anterior and posterior commissure (AC–PC line), were recorded over 5 minutes. The same EPI was applied for a second time with the prescan normalization filter to account for the higher image intensity near the surface of the receiving coils.

In order to calculate a field map aiming at correcting geometric distortions in the EPI images, 34 phase and magnitude images were acquired in the same FOV by a gradient echo (GRE) sequence with TR = 488 msec, TE(1) = 4.92 msec, TE(2) = 7.38 msec, and $\alpha = 60^\circ$. Additionally, a T1-weighted 3D magnetization prepared rapid gradient echo (MPRAGE) image was acquired for each head coil, with parameters: TR = 1.9 sec, TE = 2.52 msec, inversion time (TI) = 900 msec, 176 sagittal slices, 1 mm thick each.

fMRI Data Analysis

Spatial preprocessing and data analysis were performed with SPM5 (Wellcome Centre for Cognitive Neuroscience, London, UK). Each time series was unwarped in the phase-encoding direction by using the acquired field map in order to correct geometric distortions according to Hutton et al (20) and realigned to account for possible head motion. The EPI data were subsequently coregistered to the T1-weighted anatomical image, segmented, spatially normalized, smoothed with a Gaussian filter of 6 mm full width at half maximum, and highpass filtered (cutoff period 128 sec). Preprocessed data were statistically evaluated for each individual using the general linear model. The design matrix included as regressors the two tapping responses, modeled by a canonical hemodynamic response function, as well as the six realignment parameters of the rigid body transformation as effects of no interest. A region of interest (ROI) analysis was conducted for the primary motor cortex (M1), an area comprising the primary visual cortex V1 and the secondary visual cortex V2 (subsumed under V1-V2), the contralateral thalamus, and the ipsilateral cerebellum. The M1 and V1-V2 ROIs were defined by using cytoarchitectural masks of 50% probability from ANATOMY v. 1.6 (21). The thalamic and cerebellar ROIs were selected by anatomical masks from the Automated Anatomical Labeling (AAL) software (22). The four ROIs were selected in areas of expected activation for a finger-tapping paradigm as previously reported (9,10).

Single-Subject Analysis

A single-subject analysis was carried out at the first level of SPM by calculating the *t*-values and contrast β-estimates for the highest activated voxel of each ROI for both tapping sequences. The thus obtained two sets of values for every participant (*t*-values and contrast estimates) served each as a parameter to a multivariate analysis of variance (ANOVA) over all participants with Greenhouse-Geisser correction, with main factors coil (12ch, 32ch), filter (unfiltered, filtered), and ROI (M1, V1-V2, thalamus, cerebellum), followed by post-hoc *t*-tests corrected for multiple comparisons.

Moreover, the β-image corresponding to the task execution intervals of each session was voxel-wise divided by the β-image corresponding to the session grand mean. This ratio represents the local percent signal change due to the BOLD effect and was calculated for every coil-filter combination and each participant. The thus produced images from all 36 subjects were averaged for each specific coil-filter mode. The four previously calculated ROI masks (M1, V1-V2, contralateral thalamus, and ipsilateral cerebellum) were applied on the obtained mean percent signal change image over participants of each of the four coil-filter modes. For every ROI, the voxels of the masked mean ratio images with value >0.4 which were common in all four modes were considered for further statistical analysis: the mean percent signal change derived from those voxels was assessed by an ANOVA with Greenhouse-Geisser correction and main factors coil (12ch, 32ch) and filter (unfiltered, filtered). Paired *t*-tests corrected for multiple comparisons were undertaken for the factors and interactions that proved significant for an ROI mask.

Furthermore, the β-images corresponding to the session grand mean of a specific coil-filter combination were averaged over all participants. The identical z-slices of the mean image of every coil-filter mode were extracted for visual comparison between these modes.

Second-Level Group Analysis

A group analysis was also conducted by a bidirectional comparison of the different possible coil and filtering combinations via a *t*-test over all 36 subjects in the second level full factorial model in SPM5. An ROI analysis was conducted for the same brain areas described above, using an intensity threshold of $P = 0.001$ uncorrected and an extent threshold of 10 contiguous voxels.

TSNR Analysis

The tSNR for each participant and coil-filter combination was investigated at the voxel of maximum activation for each of the four ROIs, as found by the first-level fMRI analysis. The realigned, unwarped, segmented, and normalized EPI images corresponding to the resting blocks were used, whereas the first four images were skipped to allow steady state to be reached and to avoid any ongoing BOLD effect contributions from the preceding tapping block. The tSNR was then computed as the mean over the standard deviation of the selected timepoints. An ANOVA was applied to the tSNR results over all subjects, similar to the analysis of the BOLD effect estimates.

Performance Analysis

Since the velocity of finger movements has been shown to positively affect the detected fMRI signal change at the involved brain regions (23,24), we investigated its possible fluctuations in the different conditions of the present study. Button-press recordings were available, due to technical reasons, for 27 of the 36 subjects. The mean tapping frequency was calculated for each number sequence, coil, and filtering state for every one of these subjects. A post-hoc *t*-test was performed over all these conditions.

RESULTS

BOLD Effect

Single-Subject Analysis, β-Values

The ANOVA for the BOLD-parameter β revealed a main effect for ROI ($F_{(1,35)} = 90.33$, $P < 0.001$) and for the coil used ($F_{(1,35)} = 12.94$, $P < 0.001$). ROI*filter ($F_{(1,35)} = 22.56$, $P < 0.001$) and ROI*coil*filter ($F_{(1,35)} = 3.26$, $P < 0.05$) showed significant interactions. An overview of the averaged contrast estimates is shown in Fig. 2.

Table 1 (five first columns) summarizes the results of the post-hoc *t*-tests: regarding the ROIs, they revealed a most significant higher BOLD signal magnitude for V1-V2 than for M1, for the cerebellum compared to the thalamus, for the M1 compared to the cerebellum, and for the V1-V2 compared to the thalamus. Such tests for the factor coil only indicated that the 12-channel coil yielded on average a 15% higher β than the 32-channel coil. The ROI*filter interaction showed that the application of a prescan normalization filter improved the β-values for the subcortical ROIs over both coils, but deteriorated them for the cortical ones. Investigating the ROI*coil*filter interaction allowed for a more detailed description of each factor's impact: without filtering no significant differences were found between the two head coils for the cortical regions, while the 12-channel array seemed superior to the 32-channel array for the thalamus by 45% and the cerebellum by 61%. Apparently, the higher suitability of the head coil with the lesser receiving channels for the deeper brain areas led to its aforementioned overall higher contrast estimates β. The 32-channel coil profited from filtering in the subcortical regions (thalamus: +42%; cerebellum: +47%) at the expense of the cortical ones (M1: −26%; V1-V2: −24%). The BOLD effect measured with the 32-channel array at the subcortical regions after filtering was comparable to that measured with the 12-channel array without filtering.

Single-Subject Analysis, t-Values

The ANOVA of the *t*-values obtained from the single-subjects analyses indicated no significant differences

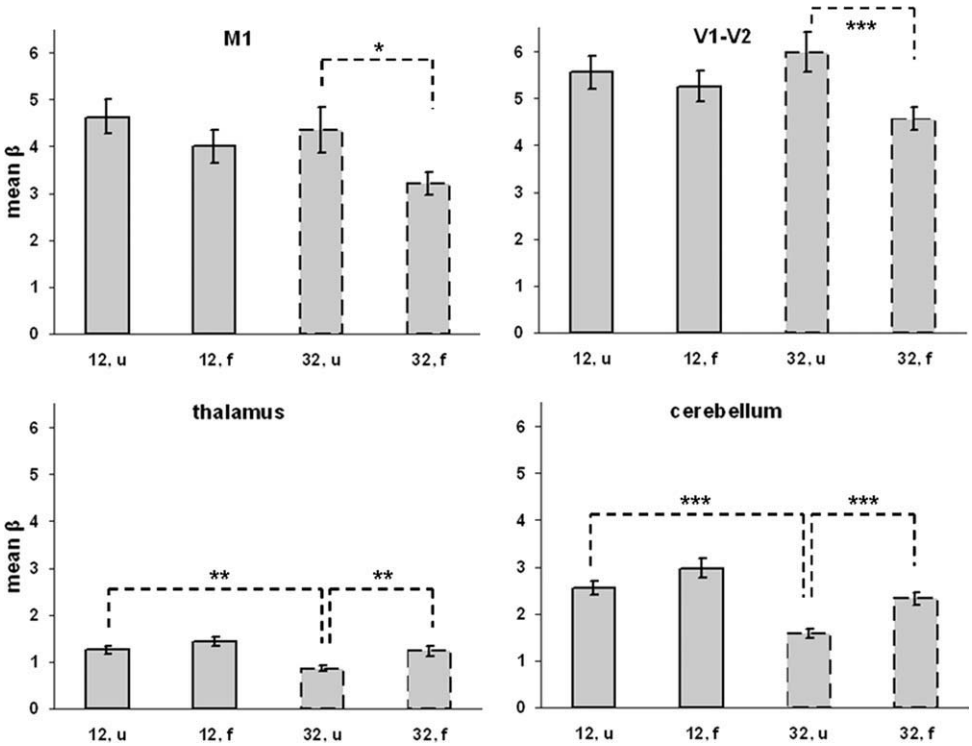

Figure 2. Mean contrast estimate β over all 36 subjects and its standard error at the voxel of maximum activation for each ROI location, head coil, and filtering condition. Significant ROI*coil*filter interactions are indicated by a dashed line. *$P < 0.05$; **$P < 0.01$; ***$P < 0.001$. f and u stand for filtered and unfiltered, respectively.

Table 1
Results of the Post-hoc *t*-Tests for the Mean β and *t*-Values of the First Level of the SPM Analysis as well as for the Mean tSNR Over All Subjects

			β		*t*		tSNR	
Factor	Comparison	df	T	$P \leq$	T	$P \leq$	T	$P \leq$
Coil	32ch > 12ch	287	−4.16	0.001	3.70	0.001	10.29	0.001
Filter	f > u	287	—	—	—	—	2.81	0.01
ROI	V1-V2 > M1	143	5.40	0.001	13.85	0.001	−0.30	ns
	cerebellum > thalamus	143	13.50	0.001	23.49	0.001	−1.01	ns
	M1 > cerebellum	143	8.76	0.001	1.01	ns	−2.17	ns
	V1-V2 > thalamus	143	23.11	0.001	27.65	0.001	−3.05	0.05
ROI*coil	M1, 32ch > M1, 12ch	71	—	—	1.86	ns	—	—
	V1-V2, 32ch > V1-V2, 12ch	71	—	—	3.06	0.05	—	—
	thalamus, 32ch > thalamus, 12ch	71	—	—	0.50	ns	—	—
	cerebellum, 32ch > cerebellum, 12ch	71	—	—	1.40	ns	—	—
ROI*filter	M1, f > M1, u	71	−3.75	0.001	—	—	—	—
	V1-V2, f > V1-V2, u	71	−3.53	0.01	—	—	—	—
	thalamus, f > thalamus, u	71	3.47	0.01	—	—	—	—
	cerebellum, f > cerebellum, u	71	6.12	0.001	—	—	—	—
ROI*coil*filter	M1, 32ch, u > M1, 12ch, u	35	−0.59	ns	—	—	—	—
	V1-V2, 32ch, u > V1-V2, 12ch, u	35	0.92	ns	—	—	—	—
	thalamus, 32ch, u > thalamus, 12ch, u	35	−3.77	0.01	—	—	—	—
	cerebellum, 32ch, u > cerebellum, 12ch, u	35	−8.95	0.001	—	—	—	—
	M1, 32ch, f > M1, 32ch, u	35	−3.15	0.05	—	—	—	—
	V1-V2, 32ch, f > V1-V2, 32ch, u	35	−3.84	0.001	—	—	—	—
	thalamus, 32ch, f > thalamus, 32ch, u	35	3.68	0.01	—	—	—	—
	cerebellum, 32ch, f > cerebellum, 32ch, u	35	9.06	0.001	—	—	—	—
	thalamus, 32ch, u > thalamus, 12ch, f	35	−0.24	ns	—	—	—	—
	cerebellum, 32ch, u > cerebellum, 12ch, f	35	−1.80	ns	—	—	—	—

P-values are Bonferroni-corrected.
df: degrees of freedom; f: filtered; u: unfiltered; — : the corresponding factor was not found significant by ANOVA.

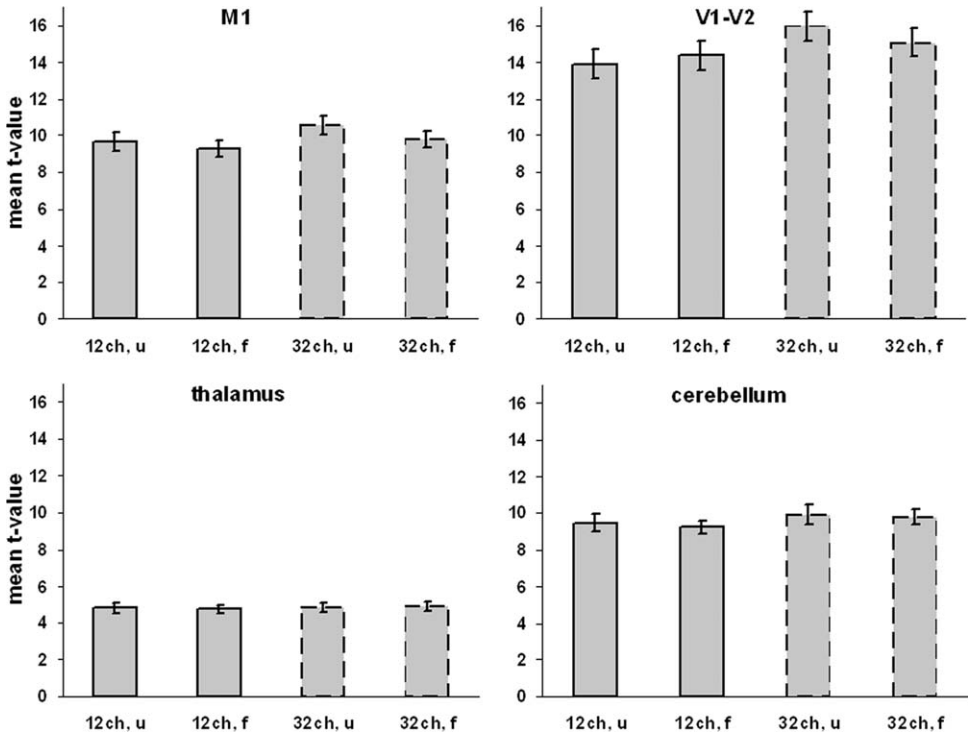

Figure 3. Mean *t*-values and their standard error over all 36 subjects at the voxel of maximum activation for each ROI location, head coil and filtering condition. f and u stand for filtered and unfiltered, respectively.

for filtering but a main effect for the factors ROI ($F_{(1,35)} = 117.74$, $P < 0.001$) and coil ($F_{(1,35)} = 4.74$, $P < 0.05$) as well as the ROI*coil interaction ($F_{(1,35)} = 3.52$, $P < 0.05$).

Post-hoc analysis (Table 1, sixth and seventh columns) for the ROIs confirmed the BOLD effect differences indicated by the β-values within the various cortical and subcortical ROIs, although activation in M1 was not significantly higher than in the cerebellum. The post-hoc *t*-tests for the coils showed on average better results for the 32-channel coil, which amounted to 7%. A more detailed inspection, considering the ROI*coil interaction, suggested that the advantage of the 32-channel array was restricted to the visual cortex V1-V2, with a 10% higher *t*-value than for the 12-channel array, while M1 showed a positive trend also (by 7%). The averaged *t*-values over all subjects are shown in Fig. 3.

Percent Signal Change

The significant results of the ANOVA for each thresholded ROI mask are presented in Table 2. Figure 4 illustrates the mean value in each mask for every coil-filter mode of the mean percent signal change over all participants. At M1, the statistical analysis showed a main effect for the filter only ($F_{(1,35)} = 48.28$, $P < 0.001$). The following post-hoc *t*-test revealed 6% higher fMRI activation without using the prescan normalization filter.

Table 2
Results of the Post-hoc *t*-Tests for the Mean Percent Signal Change in Each Thresholded ROI Mask

				% s.c.	
	Factor	Comparison	df	T	$P \leq$
M1	filter	f > u	71	−7.78	0.001
V1-V2	coil	32ch > 12ch	1545	17.58	0.001
	filter	f > u	1545	−9.68	0.001
	coil*filter	32ch, u > 12ch, u	772	19.93	0.001
		32ch, f > 32ch, u	772	−12.81	0.001
		12ch, f > 12ch, u	772	−0.03	ns
		32ch, f > 12ch, f	772	6.33	0.001
thalamus	filter	f > u	9	4.61	0.001
cerebellum	coil	32ch > 12ch	231	−3.82	0.001
	filter	f > u	231	−6.46	0.001

Only the significant factors and interactions of the ANOVA are presented for each ROI. *P* values are Bonferroni-corrected.
df: degrees of freedom; % s.c: percent signal change; f: filtered; u: unfiltered.

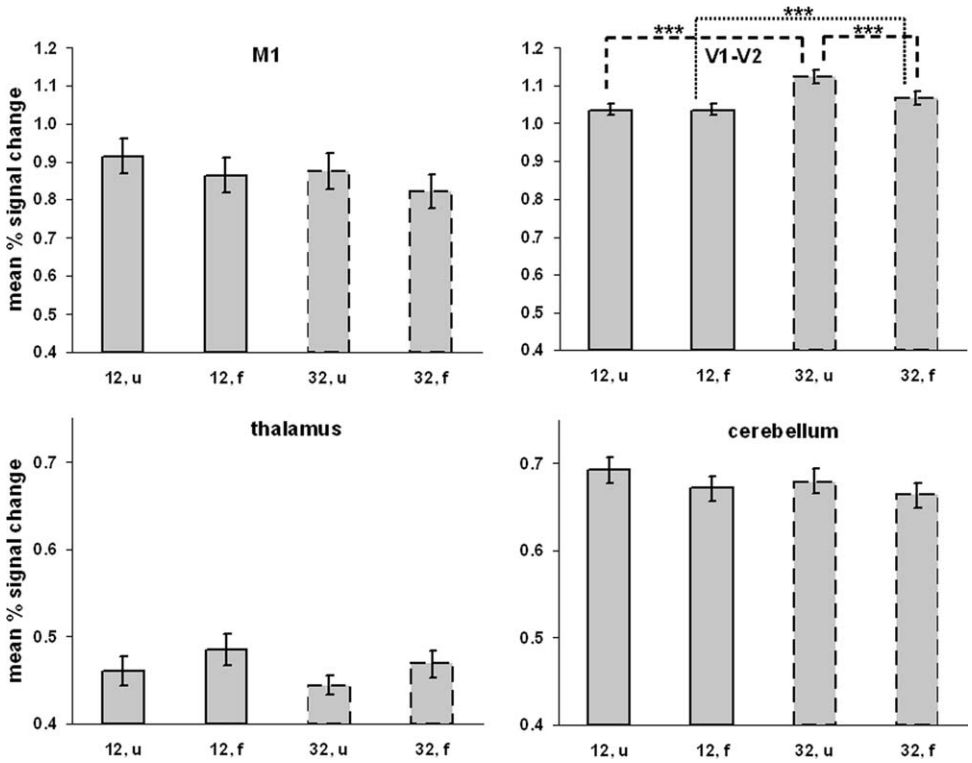

Figure 4. Mean value and standard error in every thresholded ROI mask of the mean percent signal change over all 36 subjects for each head coil and filtering condition. Significant ROI*coil*filter interactions are indicated by a dashed line. ***$P <$ 0.001. f and u stand for filtered and unfiltered, respectively.

The ANOVA for V1-V2 yielded $F_{(1,772)} = 190.72$, $P <$ 0.001 for the factor coil; $F_{(1,772)} = 62.86$, $P < 0.001$ for the factor filter; and $F_{(1,772)} = 238.27$, $P < 0.001$ for the coil*filter interaction. Post-hoc *t*-testing showed that the 32-channel coil recorded a 6% higher value than the 12-channel coil and that the filter application lowered by 3% the detected activation in this ROI. The coil*filter interaction underlined that the 32-channel array detected the most activation for every filtering condition and revealed that this array was predominantly affected by the filter application.

The ANOVA for the thalamus showed that only the filter application was a significant factor ($F_{(1,4)} =$ 13.08, $P < 0.05$), increasing by 5% the detected activation according to the paired *t*-test.

According to the ANOVA for the cerebellar ROI, both factors coil ($F_{(1,115)} = 14.58$, $P < 0.001$) and filter ($F_{(1,115)} = 37.05$, $P < 0.001$) were significant. After *t*-testing, the percent signal change was 2% higher for the 12-channel coil and 3% higher without the prescan normalization filtering.

Sensitivity Maps

An identical image slice of the fMRI signal mean within a session, averaged over subjects, that includes parts of the thalamic and visual ROIs, is presented in Fig. 5 for the various coil-filter modes studied. Each picture represents the spatial dependence of the fMRI sensitivity in the given brain slice for a specific coil-filter combination. The 32-channel coil exhibits the highest fMRI sensitivity in the peripheral anterior and posterior regions and the least sensitivity in the central brain regions without filtering (Fig. 5a). Prescan normalization filtering evened out the sensitivity's position dependency for this array (Fig. 5b), yet the values attained in most gray matter areas were low compared to the unfiltered condition of the 12-channel array (Fig. 5c). The filter application on the 12-channel coil (Fig. 5d) had a much milder smoothening effect on the sensitivity values, which were more homogeneous in the unfiltered case anyway.

Second-Level Group Analysis

Comparing the two head coils without filtering revealed a higher recorded activation of the right anterior cerebellum ([18 −48 −24], T = 5.38) and of the left thalamus ([15 −21 6], T = 3.26) by the 12-channel coil (Fig. 6a), in accordance with the statistical assessment of the contrast estimates β. The 32-channel coil recorded more activation of the right cuneus ([21 −87 9], T = 3.55) (Fig. 6b), corroborating the eligibility of this head coil for the visual cortex, as suggested by the statistical analysis of the *t*-values. All [x y z] coordinates are given in MNI space (Montreal Neurological Institute). Comparing the two filtering conditions of each head coil separately showed distinctive results: Applying or not the normalization filter on the 12-channel array did not seem to affect its fMRI detection. However, the filter application on the 32-channel array increased the recorded BOLD effect of the left thalamus ([−12 −21 9], T = 3.54) and of the right anterior cerebellum ([21 −48 −24], T = 4.33) (Fig. 6c)

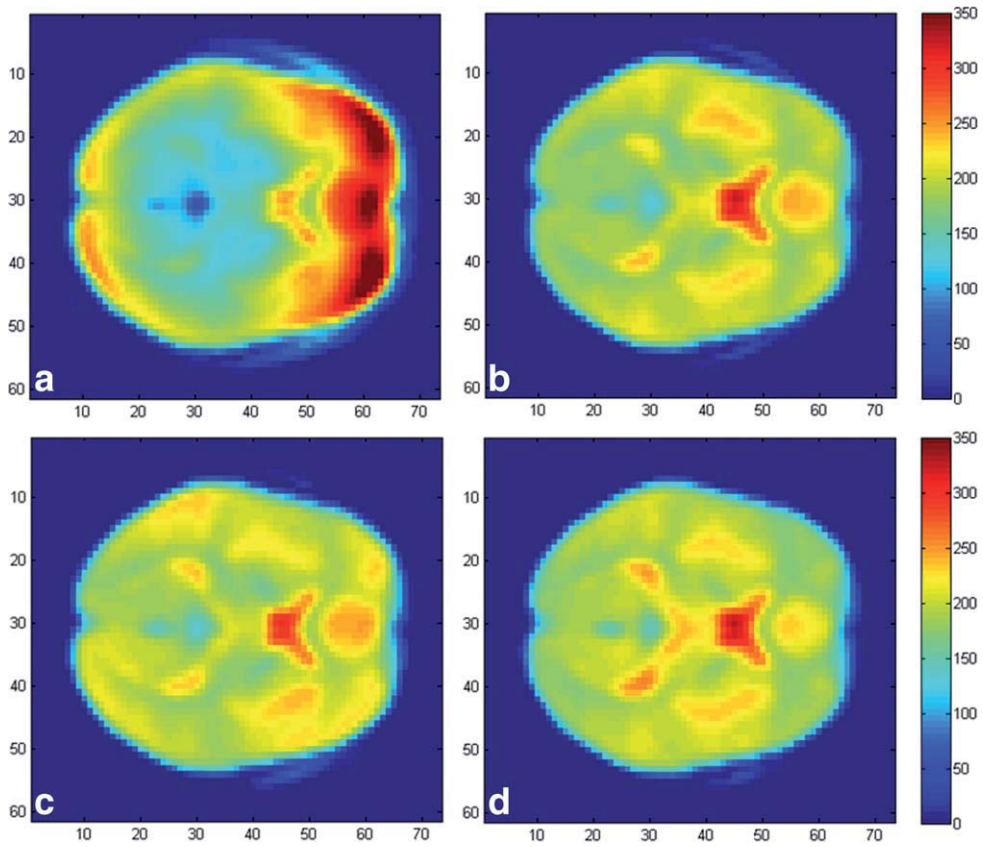

Figure 5. A map of fMRI sensitivity averaged over all participants, which includes parts of the thalamic and visual ROIs, for each coil-filter combination. **a:** 32-channel coil, unfiltered; **b:** 32-channel coil, filtered; **c:** 12-channel coil, unfiltered; **d:** 12-channel coil, filtered.

compared to the unfiltered condition of this array, confirming the results of the β values evaluation. No differences in activation occurred by applying the normalization filter on both array coils. Comparing the 32-channel coil, filtered, to the filtered or unfiltered 12-channel coil produced no significant activation differences either.

TSNR

The calculated tSNR for each ROI, coil, and filter combination is depicted in Fig. 7 as a mean over all participants. An ANOVA showed significant effects for the coil selection, filtering condition, and ROI location ($F_{(1,35)} = 72.59$, $P < 0.001$; $F_{(1,35)} = 8.62$, $P < 0.01$; $F_{(1,35)} = 3.13$, $P < 0.05$, respectively). Post-hoc *t*-testing (Table 1, last two columns) yielded an overall 38% higher tSNR for the 32-channel coil. The tSNR over all regions and coils improved also by 8% on average by using a prescan normalization filter. A significant difference in tSNR for the compared ROI pairs occurred only between the visual cortex and the thalamus (17%).

Performance

Post-hoc testing revealed no distinction in mean tapping frequency between the coils ($T_{(53)} = 0.19$, ns), thus suggesting that the brain activation was similar for both arrays and underlining the legitimacy of comparing them. The *t*-test for the two different tapping sequences over all coil and filtering conditions showed a highest significant mean tapping frequency increase for the easier sequence ($T_{(26)} = 5.10$, $P < 0.001$), as expected. Nevertheless, the corresponding SPM two-sample *t*-test indicated no significant BOLD effect differences between the tapping sequences. This comparison suggests that neither head coil could discern any differences in brain activation related to the tapping velocity for this paradigm.

DISCUSSION

The investigation of the BOLD effect, according to the statistical analysis of the parameters β calculated for the voxels of maximum activation, suggested no differences between the two head coils for regions near the arrays surface and demonstrated a higher adequacy of the 12-channel coil for studying central brain areas. Prescan normalization filtering increased the BOLD signal magnitude detected from the 32-channel coil for these areas but would not be recommended for the cortical ROIs. This filtering method compensates for RF field inhomogeneities of the receiving coils by adjusting the acquired images to the assumed homogeneous sensitivity of the body coil. Due to B1-field inhomogeneities this assumption is not completely fulfilled; therefore, the images acquired

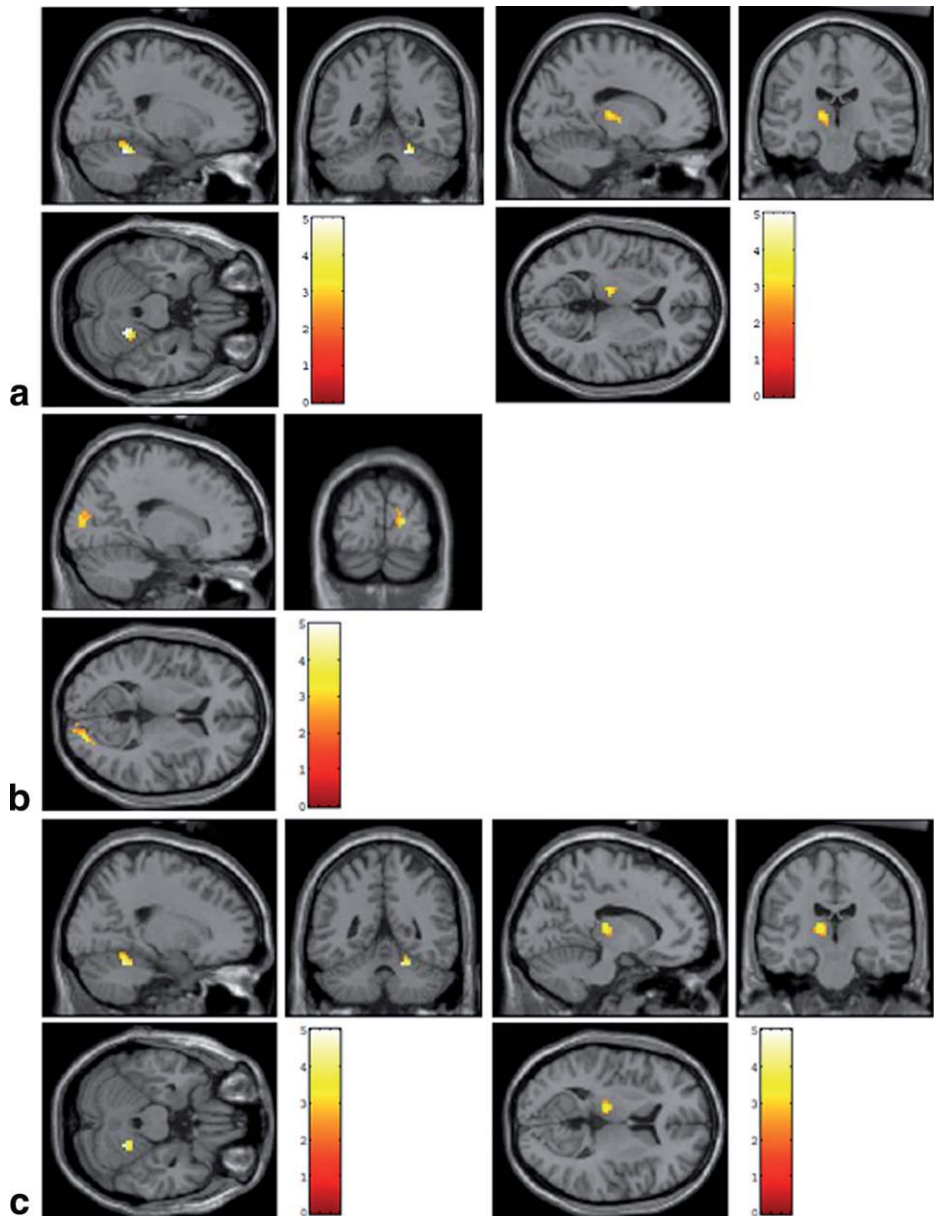

Figure 6. Significant results of the second level *t*-tests ($P = 0.001$). **a**: 12-channel coil, unfiltered > 32ch-coil, unfiltered [18 −48 −24], T = 5.38; [15 −21 6], T = 3.26. **b**: 32-channel coil, unfiltered > 12-channel coil, unfiltered [21 −87 9], T = 3.55. **c**: 32-channel coil, filtered > 32-channel coil, unfiltered [−12 −21 9], T = 3.54; [21 −48 −24], T = 4.33.

from the body coil exhibit a signal intensity loss towards their edges. As shown previously (25), RF transmit inhomogeneities cause local flip angle deviations which are stronger in cortical than in subcortical brain regions at 3 T. Such spatial irregularities are not corrected by the prescan normalization procedure and are presumably reflected on the observed increase of the BOLD parameters near the brain center and their decrease at the cortex after this kind of image homogenization filtering.

Regarding the mean *t*-values corresponding to the voxels of maximum activation from the first-level analysis, the 32-channel head coil demonstrated slightly better results near its surface, especially for the visual cortex, but there was no evidence of improvement for the more distant brain areas. According to the percent signal change over the entire ROI masks, the 32-channel coil was again better in fMRI terms for the visual cortex and worse for the cerebellum, and prescan normalization filtering decreased the BOLD effect detected from the cortical and cerebellar regions while increasing it at the thalamus.

The group analysis approach via a two sample *t*-test at the second level of SPM confirmed the fMRI eligibility of the 32-element array for the visual cortex and of the 12-element array for the thalamus and cerebellum, as well as the positive impact of the filter application on the 32-element array for the central brain regions. Observations from the fMRI sensitivity maps were in general agreement with the outcome of the SPM analyses.

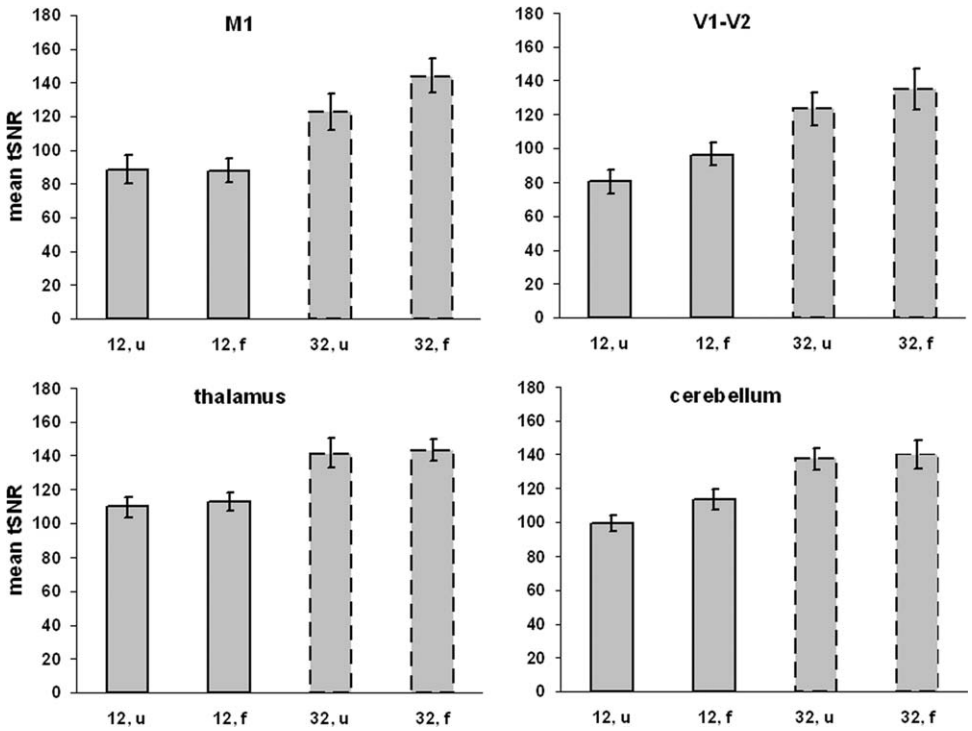

Figure 7. Mean tSNR over all 36 subjects and its standard error at the voxel of maximum activation for each ROI location in the brain, each head coil, and each filtering condition. f and u stand for filtered and unfiltered, respectively.

Our results corroborate the indication of Kahn et al (6) about higher BOLD detection from the 32-channel array at the visual cortex but agree only partially with results of Fellner et al (7) about the detection differences between the two array coils at the motor cortex. This might be due to the different evaluating methods (vendor-specific software) and different motor cortex masks they used, the different spatial resolution, the lower B_0 field of 1.5 T, and the much smaller group of seven subjects that they studied. The comparability of our fMRI results to those reported by Albrecht et al (8) is limited not only by the fact that their differently constructed 32-channel coil was compared to an 8-channel coil, both designed by another manufacturer, but also by the parallel acceleration they used and the mainly different brain regions they studied. However, they also suggested that their 32-channel coil would be advantageous for cortical fMRI studies but disadvantageous for deeper brain regions.

Inspecting the tSNR of the same voxels assessed by the fMRI investigation revealed higher values for the 32-channel coil, in line with the high SNR of a 32-channel array reported by Wiggins et al (4,5). Applying a prescan normalization filter also increased the observed tSNR over both coils, presumably because this kind of filtering evened out the original image intensity inhomogeneities. Such image intensity enhancements near the head surface were more pronounced for the coil with the higher number of RF channels. The fact that its casing has smaller dimensions and thus its smaller-sized elements lie closer to the skull might explain its overall surface coil-like behavior. The majority of its RF channels are situated in the dorsal part of the helmet, which might account for the observed higher BOLD signal reception from occipital brain regions. The 12 receiving elements of the head matrix coil have bigger dimensions and are symmetrically arranged around the head, presumably accounting for the observed higher signal homogeneity of this array.

Interestingly, the detected BOLD effect magnitude did not convincingly seem to benefit from the increased signal sensitivity attributed to the 32-channel array by the present tSNR evaluation. The tSNR was calculated using the resting scans, to avoid any influence from activation, during which the physiological noise due to subject movement was smaller than during the task-executing periods. The consequent reduction of the ratio physiological-to-thermal noise might explain the discrepancy between tSNR and BOLD activation parameters. Moreover, the scans corresponding to activation blocks were smoothed, as recommended for most fMRI applications in order to render the errors more normal in their distribution and ensure the validity of inferences based on parametric tests (26). Smoothing, however, might reduce the voxel values actually considered for statistical inference, leading to reduction of the resulting brain activation parameters.

It has to be mentioned that the results obtained in this fMRI study have to be interpreted for the spatial resolution used, which is the most common one for fMRI measurements. For a higher image resolution the ratio of physiological-to-thermal noise could be decreased (14), leading to a higher BOLD signal magnitude. In the present work we restricted ourselves to the standard settings of both coils. Parallel imaging may yield better BOLD results for the 32-channel

than for the 12-channel coil, as has been reported for other MRI-sequences such as diffusion tensor imaging (DTI) (27).

The present study was carried out on a specific MRI apparatus, with commercial head coils and filtering methods. A generalization of our results for other MRI systems should be performed with care. However, similar activation trends might appear for coils and filters of similar design as the ones surveyed here.

It is also noteworthy that both the filtered and unfiltered EPI time series of the same session were available during application of the prescan normalization filter. One might consider using these data to compare functional activation between the two filtering conditions for the same head coil in order to reduce variance and increase the statistical power of the analysis. The goal of the present study, however, was to compare the activation between the possible combinations of coils and filtering conditions. As the fMRI data from the different coils were inevitably acquired during different sessions, the filtered and unfiltered time series were deliberately acquired during different sessions too, in order to have the same variance in each term of the comparison.

In conclusion, at 3 T and a medium spatial resolution, a commercial phased-array head coil with 32 receiving elements seemed advantageous for detecting the fMRI signal magnitude of the visual cortex. However, a commercial 12-channel head matrix coil recorded higher activation at the subcortical regions of the thalamus and cerebellum. Image signal homogenization by prescan normalization would only be advised for fMRI studies focused on central brain regions, since its application might decrease the cortical BOLD signal magnitude.

ACKNOWLEDGMENT

The authors thank Chloe Hutton and Silke Anders for useful advice.

REFERENCES

1. Wright SM, Wald LL. Theory and application of array coils in MR spectroscopy. NMR Biomed 1997;10:394–410.
2. Lin CS, Rajan SS, Gold J. A novel multi-segment surface coil for neuro-functional magnetic resonance imaging. Magn Reson Med 1998;39:164–168.
3. de Zwart JA, Ledden PJ, van Gelderen P, Bodurka J, Chu R, Duyn JH. Signal-to-noise ratio and parallel imaging performance of a 16-channel receive-only brain coil array at 3.0 Tesla. Magn Reson Med 2004;51:22–26.
4. Wiggins GC, Triantafyllou C, Potthast A, Reykowski A, Nittka M, Wald LL. 32-channel 3 Tesla receive-only phased-array head coil with soccer-ball element geometry. Magn Reson Med 2006;56:216–223.
5. Wiggins GC, Polimeni JR, Potthast A, Schmitt M, Alagappan V, Wald LL. 96-Channel receive-only head coil for 3 Tesla: design optimization and evaluation. Magn Reson Med 2009;62:754–762.
6. Kahn I, Wiggins CJ, Wiggins G, et al. High-resolution human functional MRI: feasibility and specificity at high (3T) and ultra-high (7T) fields. In: Proc Joint Annual Meeting ISMRM-ESMRMB, Berlin; 2007:1927.
7. Fellner C, Doenitz C, Finkenzeller T, Jung EM, Rennert J, Schlaier J. Improving the spatial accuracy in functional magnetic resonance imaging (fMRI) based on the blood oxygenation level dependent (BOLD) effect: benefits from parallel imaging and a 32-channel head array coil at 1.5 Tesla. Clin Hemorheol Microcirc 2009;43:71–82.
8. Albrecht J, Burke M, Haegler K, et al. Potential impact of a 32-channel receiving head coil technology on the results of a functional MRI paradigm. Clin Neuroradiol 2010;20:223–229.
9. Dhamala M, Pagnoni G, Wiesenfeld K, Zink CF, Martin M, Berns GS. Neural correlates of the complexity of rhythmic finger tapping. Neuroimage 2003;20:918–926.
10. Lotze M, Erb M, Flor H, Huelsmann E, Godde B, Grodd W. fMRI evaluation of somatotopic representation in human primary motor cortex. Neuroimage 2000;11:473–481.
11. de Zwart JA, van Gelderen P, Kellman P, Duyn JH. Application of sensitivity-encoded echo-planar imaging for blood oxygen level-dependent functional brain imaging. Magn Reson Med 2002;48: 1011–1020.
12. Lutcke H, Merboldt KD, Frahm J. The cost of parallel imaging in functional MRI of the human brain. Magn Reson Imaging 2006; 24:1–5.
13. Kruger G, Kastrup A, Glover GH. Neuroimaging at 1.5 T and 3.0 T: comparison of oxygenation-sensitive magnetic resonance imaging. Magn Reson Med 2001;45:595–604.
14. Triantafyllou C, Hoge RD, Krueger G, et al. Comparison of physiological noise at 1.5 T, 3 T and 7 T and optimization of fMRI acquisition parameters. Neuroimage 2005;26:243–250.
15. Kruger G, Glover GH. Physiological noise in oxygenation-sensitive magnetic resonance imaging. Magn Reson Med 2001;46: 631–637.
16. Petridou N, Loew M, Bandettini PA. S/N and fMRI sensitivity. In: Proc SPIE – The International Society for Optical Engineering, vol. 4682. San Jose, CA; 2002:746–754.
17. Parrish TB, Gitelman DR, LaBar KS, Mesulam MM. Impact of signal-to-noise on functional MRI. Magn Reson Med 2000;44: 925–932.
18. Roemer PB, Edelstein WA, Hayes CE, Souza SP, Mueller OM. The NMR phased array. Magn Reson Med 1990;16:192–225.
19. Bernstein MA, Huston J 3rd, Ward HA. Imaging artifacts at 3.0T. J Magn Reson Imaging 2006;24:735–746.
20. Hutton C, Bork A, Josephs O, Deichmann R, Ashburner J, Turner R. Image distortion correction in fMRI: a quantitative evaluation. Neuroimage 2002;16:217–240.
21. Eickhoff SB, Stephan KE, Mohlberg H, et al. A new SPM toolbox for combining probabilistic cytoarchitectonic maps and functional imaging data. Neuroimage 2005;25:1325–1335.
22. Tzourio-Mazoyer N, Landeau B, Papathanassiou D, et al. Automated anatomical labeling of activations in SPM using a macroscopic anatomical parcellation of the MNI MRI single-subject brain. Neuroimage 2002;15:273–289.
23. Rao SM, Bandettini PA, Binder JR, et al. Relationship between finger movement rate and functional magnetic resonance signal change in human primary motor cortex. J Cereb Blood Flow Metab 1996;16:1250–1254.
24. Riecker A, Wildgruber D, Mathiak K, Grodd W, Ackermann H. Parametric analysis of rate-dependent hemodynamic response functions of cortical and subcortical brain structures during auditorily cued finger tapping: a fMRI study. Neuroimage 2003; 18:731–739.
25. Lutti A, Hutton C, Finsterbusch J, Helms G, Weiskopf N. Optimization and validation of methods for mapping of the radiofrequency transmit field at 3T. Magn Reson Med 2010;64: 229–238.
26. Friston K, Karl F, John A, Stefan K, Thomas N, William P. Statistical parametric mapping. London: Academic Press; 2007. p 10–31.
27. Stieltjes B, Klein J, Hyman B, Naul LG, Runge V, Essig M. Reproducible quantification of fiber integrity profiles in the cingulum and the fornix using an experimental 32 channel head coil. In: Proc 16th Annual Meeting ISMRM, Toronto; 2008:1842.